Biomaterials 33 (2012) 1090–1096

Contents lists available at SciVerse ScienceDirect

Biomaterials

journal homepage: www.elsevier.com/locate/biomaterials

Simultaneous electrochemical detection of multiple analytes based on dual signal amplification of single-walled carbon nanotubes and multi-labeled graphene sheets

Lijuan Bai, Ruo Yuan*, Yaqin Chai, Ying Zhuo, Yali Yuan, Yan Wang

Education Ministry Key Laboratory on Luminescence and Real-Time Analysis, College of Chemistry and Chemical Engineering, Southwest University, Chongqing 400715, PR China

ARTICLE INFO

Article history:
Received 27 September 2011
Accepted 6 October 2011
Available online 5 November 2011

Keywords:
Electrochemical aptasensor
Simultaneous detection
Signal amplification
Multi-labeled graphene sheets

ABSTRACT

In this work, a sandwich-type electrochemical aptasensor for simultaneous sensitive detection of platelet-derived growth factor (PDGF) and thrombin is fabricated. Reduced graphene oxide sheets (rGS) are used as matrices to immobilize the redox probes, which are subsequently coated with platinum nanoparticles (PtNPs) to form the PtNPs-redox probes-rGS nanocomposites. With the employment of the as prepared nanocomposites, a signal amplification strategy was described based on bienzyme (glucose oxidase and horseradish peroxidase) modified PtNPs-redox probes-rGS nanocomposites as the tracer labels for secondary aptamers (Apt II) through sandwiched assay. Gold nanoparticles functionalized single-walled carbon nanotubes (AuNPs@SWCNTs) as the biosensor platform enhance the surface area to capture a large amount of primary aptamers (Apt I), thus amplifying the detection response. The experiment results show that the multi-labeled PtNPs-redox probes-rGS nanocomposites display satisfying electrochemical redox activity and highly electrocatalytic activity of PtNPs and bienzyme, which exhibit high sensitivity for detection of proteins. The linear range of PDGF is 0.01–35 nM with a detection limit of 8 pM, while the linear ranges from 0.02 to 45 nM and a detection limit of 11 pM for thrombin are obtained.

1. Introduction

It is well known that there are manifold regulatory factors in human body holding different functions in vital movement. For instance, platelet-derived growth factor (PDGF) is an important growth factor protein in human platelets that regulates cell growth and division toward fibroblasts, smooth muscle cells and glial cells [1], while thrombin is a extracellular serine protease that plays crucial roles in the blood coagulation cascade, thrombosis and haemostasis [2,3]. Thus, precise and sensitive evaluation of these proteins in biological samples will be substantial for disease diagnosis. Aptamer-based assay technologies, such as fluorescence [4], chemiluminescence [5], colorimetric [6] and electrochemistry [7] have been reported for individual detection of various analytes. Among these methods, electrochemical assays hold great promise for their portability, low cost and high sensitivity [8–11]. Compared with the traditional single analyte assay, the simultaneous multiplex assay is more efficient in clinical application since it can shorten analytical time and decrease detection cost. Up to now, simultaneous electrochemical detection of multiple analytes using aptamer-based assay has rarely been reported. Wang and co-workers [12] described a reusable label-free biosensor based on an integrated aptamer for parallel detection of adenosine triphosphate (ATP) and thrombin by using electrochemical impedance spectroscopy and cyclic voltammetry. Zhang's group [13] developed a dual-functional aptamer DNA sequence for the detection of adenosine and thrombin by coupling the enhancement of bio-barcode technology and anodic stripping voltammetry. Our group [14] has fabricated functionalized Pt hollow nanospheres as trace labels for simultaneous electrochemical immunoassay by using tumor markers carcinoembryonic antigen (CEA) and α-fetoprotein (AFP) as model systems. However, to the best of our knowledge, simultaneous electrochemical detection of PDGF and thrombin using aptamer-based sensor (aptasensor) have not been reported.

Increasing interests have been focused on graphene due to its unique structure and electronic properties, such as large accessible surface area, excellent electronic transport properties and exceptional thermal stability [15–18], holding great promise in the applications of catalytic support for electron transfer and for signal amplification of electrical biosensing [19–21]. However, due to the

* Corresponding author. Tel./fax: +86 23 68252277.
E-mail address: yuanruo@swu.edu.cn (R. Yuan).

0142-9612/$ – see front matter © 2011 Elsevier Ltd. All rights reserved.
doi:10.1016/j.biomaterials.2011.10.012

strong π-π stacking tendency between the nanosheets, unmodified graphene sheets are apt to aggregate and inhibit the advantages of the specific properties when they are directly exposed to the biological system [22], thus a variety of biomaterial-functionalized graphene have been extensively applied [23–25]. Here we choose electroactive and biocompatible redox probes-toluidine blue (Tb) and ferrocene (Fc) attached with reduced graphene oxide sheets (rGS) respectively, which overcome the aggregation and provide qualitative foundation for multiple detection. On the other hand, platinum nanoparticles (PtNPs) are satisfactory biocompatible nanomaterials because of their strong adsorption ability, good conductivity and excellent electrocatalytic activity to hydrogen peroxide [26,27]. Thus, PtNPs were modified on the surface of redox probes labeled rGS to form the PtNPs-redox probes-rGS nanocomposites, which not only accelerate the electron transfer but also facilitate the immobilization of enzyme and secondary aptamers (Apt II) with favorable catalysis activity and bioactivity.

Herein, we developed an electrochemical assay for simultaneous detection of PDGF and thrombin using gold nanoparticles functionalized single-walled carbon nanotubes (AuNPs@SWCNTs) as the sensor platform and distinguishable electrochemical signal tags as tracers. AuNPs is a kind of excellent nanomaterials with favorable biocompatibility, good conductivity and high affinity, which offers an active interface to absorb abundant aptamers by chemical absorption between AuNPs and $-NH_2$ of aptamers [28,29]. SWCNTs with special structural feature and unique electronic properties [30] promote electron transfer and increase the surface area of AuNPs to capture a large amount of primary aptamers (Apt I). Redox probes Tb and Fc were initially modified onto rGS, respectively, and the synthesized PtNPs-redox probes-rGS nanocomposites were then served as carriers for bienzyme (glucose oxidase and horseradish peroxidase) and corresponding secondary aptamers (Apt II)—PDGF binding aptamer and thrombin binding aptamer. With the sandwich-type assay format, the aptamer-analyte complex was formed on the surface of AuNPs@SWCNTs, and the carried GOD catalyzes the reduction of glucose to generate H_2O_2, which is further reduced by HRP and PtNPs with the aid of the two independent redox probes.

2. Materials and methods

2.1. Reagents and materials

Graphene oxide was obtained from Nanjing xianfeng nano Co. (Nanjing, China). Platelet-derived growth factor (PDGF-BB), thrombin, toluidine blue (Tb), monocarboxylic ferrocene (Fc), polyethyleneimine (PEI), hexanethiol (96%, HT), L-cysteine, chitosan, gold chloride ($HAuCl_4$) and chloro platinic acid (H_2PtCl_6) were purchased from Sigma Chemical Co. (St. Louis, MO, USA). Glutaraldehyde (GA), 1-ethyl-3-(3-dimethylaminopropyl) carbodiimide hydrochloride (EDC) and N-hydroxy succinimide (NHS) were acquired from Shanghai Medpep Co. (Shanghai, China). Shortened carboxylate single-walled carbon nanotubes (SWCNTs) and dimethyl formamide (DMF) were supplied by Shenzhen Nanothch Port Co., Ltd. (Shenzhen, China). Glucose oxidase (GOD) and horseradish peroxidase (HRP) was obtained from the Shanghai Biochemical Co. (China). Trishydroxymethylaminomethane hydrochloride (Tris-HCl) was purchased from Roche (Switzerland). The PDGF binding aptamer (PBA) and thrombin binding aptamer (TBA) were purchased from TaKaRa (Dalian, China), and the sequences of the oligonucleotides were as follows:

PBA: 5′-NH_2-$(CH_2)_6$-CAGGCTACGGCACGTAGAGCATCACCATGATCCTG-3′

TBA: 5′-NH_2-$(CH_2)_6$-AGTCCGTGGTAGGGCAGGTTGGGGTGACT-3′

20 mM Tris-HCl buffer (pH 7.4) contaning 140 mM NaCl, 5 mM KCl and 1 mM $MgCl_2$ was used to prepare aptamer solutions. 0.1 M phosphate buffered solutions (PBS, pH 7.4) containing 10 mM Na_2HPO_4, 10 mM KH_2PO_4 and 2 mM $MgCl_2$ was used throughout the experiment. All other chemicals were of reagent grade and used as received.

2.2. Apparatus and characterization

Cyclic voltammetry (CV), electrochemical impedance spectroscopy (EIS) and differential pulse voltammetry (DPV) measurements were carried out with a CHI 660D electrochemical workstation (Shanghai Chenhua Instrument, China). All experiments were performed in a conventional three-electrode system: a platinum wire auxiliary electrode, a saturated calomel reference electrode (SCE) and the modified glassy carbon electrode (GCE, $\Phi = 4$ mm) as working electrode. Transmission electron microscopy (TEM) images were obtained with a JEOL-JEM 2000CX transmission electron microscope (H600, Hitachi, Japan). X-ray photoelectron spectroscopy (XPS) analysis was carried out using a VG Scientific ESCALAB 250 spectrometer, using Al Kα X-ray (1486.6 eV) as the light source. The pH measurements were made with a pH meter (MP 230, Mettler-Toledo, Switzerland).

2.3. Preparation of aptamers, GOD and HRP multi-labeled PtNPs-redox probes-rGS nanocomposites

Initially, reduced graphene oxide sheets (rGS) were prepared according to reference [24] with a slight modification. 10 mL stable dispersion of exfoliated graphene oxide sheets (1 mg/mL) were mixed with 1 mL PEI (3%) and heated under reflux at 135 °C for about 3 h. The obtained black product was washed several times by double distilled water and collected by centrifugation. The synthesized rGS have abundant amino, thus, EDC and NHS were used as coupling agents to modify the rGS with Fc (Fc-rGS) by formation of an amide link between the carboxyl of Fc and the amino of rGS. Analogously, GA was served as crosslinking agent to modify rGS with Tb (Tb-rGS) by the interaction of amino between them. The Fc-rGS and Tb-rGS conjugates were gently stirred for 2 h, respectively, then centrifuged and washed twice with double distilled water to remove the unmodified redox probes.

The resulting redox probes-rGS bioconjugates were then surface-chemically modified by L-cysteine branched chitosan (CBC) to obtain the active groups of amino and thiol for attraction of nanoparticles while inhibiting the leakage of redox probes. Platinum nanoparticles-enwrapped redox probes-rGS (PtNPs-redox probes-rGS) nanocomposites were constructed using the $NaBH_4$ reduction method. Biriefly, 1 mL H_2PtCl_6 (1%) was added dropwise into 5 mL CBC protected redox probes-rGS bioconjugates and vigorously stirred for 5 min to make the negatively charged $PtCl_6^{2-}$ ions adsorbed on the CBC surface. Then, 2.5 mL $NaBH_4$ (0.1 M) solution was dropped into the mixture with stirring for 30 min, followed by centrifugation and washing with double distilled water.

Subsequently, 100 μL PBA (2 μM) was added to 5 mL colloidal PtNPs-Tb-rGS, and 100 μL TBA (2 μM) was added to 5 mL colloidal PtNPs-Fc-rGS respectively, followed by incubation at 4 °C for 12 h. Finally, 1 mg GOD and 1 mg HRP were dissolved in the PtNPs-redox probes-rGS labeled aptamers solution and incubated at 4 °C for 4 h to block the unspecified sites and prevent non-specific adsorption. After centrifugation and washing, the multi-labeled PtNPs-redox probes-rGS nanocomposites were resuspened in Tris-HCl buffer and stored at 4 °C for further use. Fig. 1A shows the schematic illustration of the preparation procedure for the multi-labeled PtNPs-redox probes-rGS nanocomposites.

2.4. Fabrication of the aptasensor

Prior to use, 1 mg activated SWCNTs were suspended in 1 mL DMF and sonicated to obtain a homogeneous black solution. Firstly, 5 μL the SWCNTs solution was dropped onto a pretreated GCE to increase the effective area of the electrode. Then the electrode was dried at room temperature and immersed into $HAuCl_4$ solution for electrochemical deposition to obtain gold nanoparticles (AuNPs). Subsequently, the formed AuNPs@SWCNTs modified electrode was submerged into the mixture solution of 2 μM PBA and 2 μM TBA for 16 h at room temperature. Then the resulting aptasensor was incubated with blocking solution (0.1 M PBS containing 1.0 mM HT) for 1 h to eliminate non-specific binding effects and block the remaining active groups. After every step, the modified electrode was thoroughly cleaned with double distilled water and PBS buffer to prevent the non-chemisorption. The finished aptasensor was stored at 4 °C when not in use.

The detection was based on the typical process for sandwiched assay. First, the aptasensor was incubated with 20 μL drop of the mixture of PDGF and thrombin standard solutions with different concentrations for 1 h at room temperature, followed by washing. Then it was further incubated with the prepared multi-labeled PtNPs-redox probes-rGS nanocomposites for 1 h at room temperature. After rinsing thoroughly with double distilled water and PBS to remove the unbound secondary aptamers, the amperometric responses of the aptasensor were recorded for the quantitative detection of PDGF and thrombin. Fig. 1B showed the schematic illustration of the stepwise procedure of the aptasensor fabrication and the corresponding catalysis amplifying principle of the bienzyme functionalized PtNPs-redox probes-rGS nanocomposites based on the sandwich assay.

2.5. Experimental measurements

Electrochemical experiments were carried out in a conventional electrochemical cell, in which a modified working electrode, a SCE reference electrode and a Pt counter electrode were used. EIS of the electrode fabrication were performed in 5 mM $K_3Fe(CN)_6$ solution containing 0.1 M KCl. CV scan was taken from −0.6 to 0.6 V (vs. SCE) at a scan rate of 100 mV/s in 0.1 M PBS (pH 7.4). DPV was performed in 0.1 M PBS (pH 7.4) containing 3.6 mM glucose to measure the amperometric responses of the aptasensor. The parameters applied were: 50 mV pulse amplitude, 50 ms pulse width, 0.2 s pulse period and voltage range from −0.6 to 0.6 V (vs. SCE).

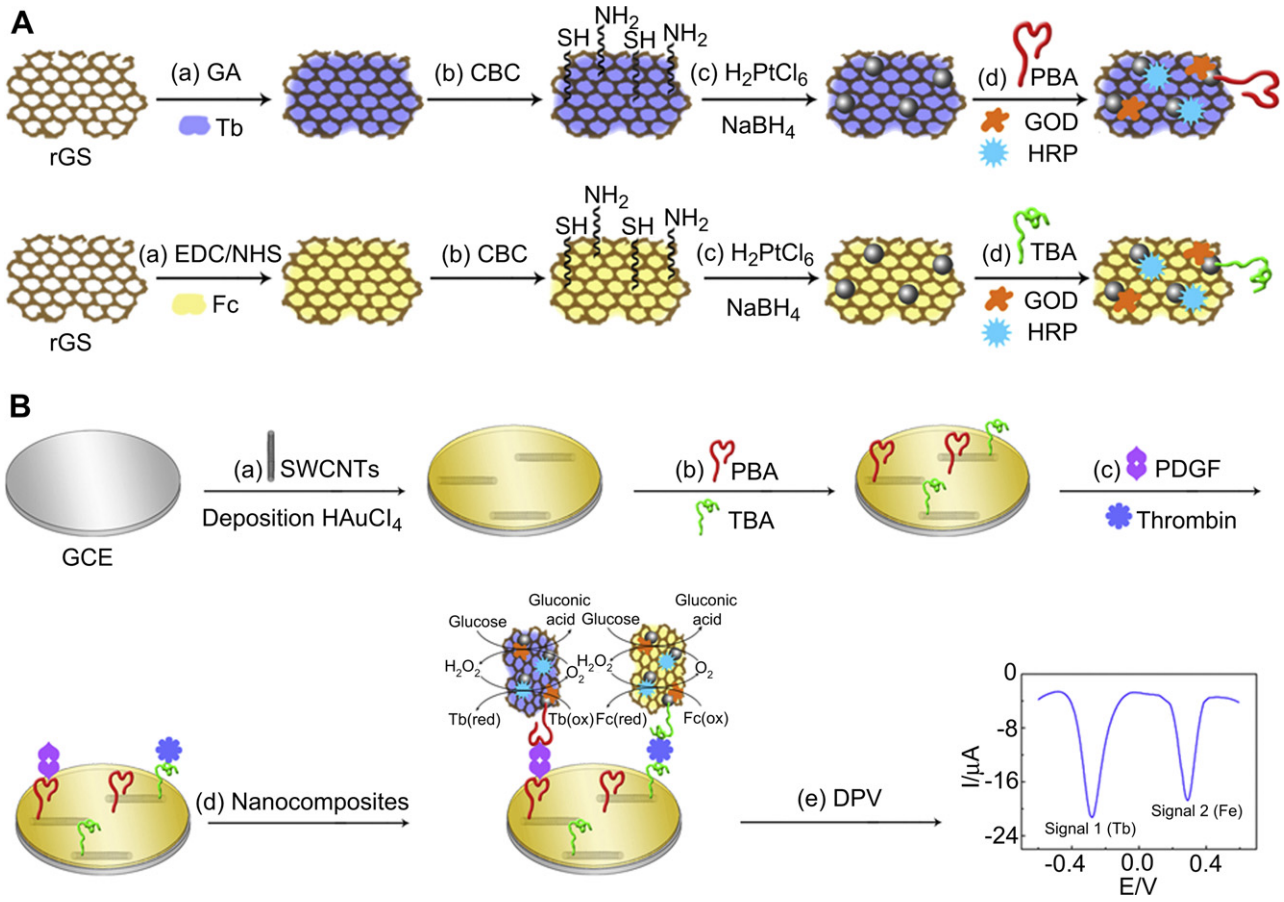

Fig. 1. (A) Preparation procedure of aptamers, GOD and HRP multi-labeled PtNPs-redox probes-rGS nanocomposites: (a) modification with redox probes, (b) coating with L-cysteine branched chitosan (CBC) to obtain active groups of amino and thiol, (c) reducing H_2PtCl_6 to form PtNPs, (d) labeled with aptamers, GOD and HRP. (B) Schematic illustration of the stepwise aptasensor fabrication process: (a) dropping of SWCNTs membrane and electrodeposition of $HAuCl_4$, (b) immobilization of Apt I, (c) reaction with analytes PDGF and thrombin, (d) incubating with multi-labeled PtNPs-redox probes-rGS nanocomposites, (e) DPV measurement of current response in PBS containing 3.6 mM glucose.

3. Results and discussion

3.1. Characteristics of the different nanomaterials

Transmission electron microscopy (TEM) images give the size and morphology of the as synthesized composites. As shown in Fig. 2a, the SWCNTs dispersed in DMF showed a homogeneous configuration and good dispersion. The lamellate and porous sheets suggested the successful preparation of rGS (Fig. 2b) and the homogeneous and dense coverage of PtNPs on the rGS could be observed in Fig. 2c. The sheet remained separated with each other without any aggregation, implying the well dispersibility of the nanocomposites in solution.

To further analyze the chemical composition of the PtNPs-redox probes-rGS nanocomposites, X-ray photoelectron spectroscopy (XPS) characterization was employed. The fully scanned spectra demonstrated the existence of C and O elements in graphene oxide and N element in the synthesized rGS (Fig. 2d). The characteristic peaks for Pt4f, S2p, C1s, N1s and O1s core level regions could be obviously observed at the PtNPs-Tb-rGS nanocomposites in Fig. 2e. The S2p core level was mainly derived from the redox probe Tb and the Pt4f doublet (72.3 eV and 75.1 eV) indicated the presence of PtNPs. In addition, higher characteristic peaks at C1s and N1s were observed, which further proved the existence of Tb. Fig. 2f showed the Pt4f, C1s, N1s, O1s and Fe2p core level regions of the PtNPs-Tb-rGS nanocomposites. It could be found that the Fe 2p core level region (710 eV and 727 eV) originated from Fc. Because of the existence of elemental oxygen in Fc, a higher characteristic peak at O1s was achieved.

3.2. Electrochemical characterization of the aptasensor

Electron-transfer resistance (R_{et}) at the electrode is an important parameter, thus electrochemical characteristics of the aptasensor was investigated by EIS measurements. It is well known that the high frequency region of the impedance plot shows a semicircle related to the redox probe $[Fe(CN)_6]^{3-/4-}$ and the semicircle diameter of EIS is equal to R_{et}. Fig. 3 illustrated the EIS of different electrodes in the presence of 5 mM $[Fe(CN)_6]^{3-/4-}$ containing 0.1 M KCl. Bare GCE had a small semicircle (R_{et} = 120 Ω, curve a), implying relatively low resistance to the redox probe dissolved in solution. When SWCNTs and AuNPs were modified onto the electrode, the resistance decreased apparently (curve b) compared with bare electrode, which attributed to the AuNPs@SWCNTs modified electrode had large effective surface area than bare GCE and promoted electron transfer. With Apt I adsorption on the surface of AuNPs@SWCNTs, the semicircle increased remarkably (R_{et} = 187 Ω, curve c) because the capture aptamers as non-electroactive properties obstructed electron transfer. After non-conductive HT was used to block non-specific sites, the resistance increased again (curve d). The resistance further increased when the electrode was incubated with PDGF and thrombin (R_{et} = 478 Ω, curve e), which attributed to the

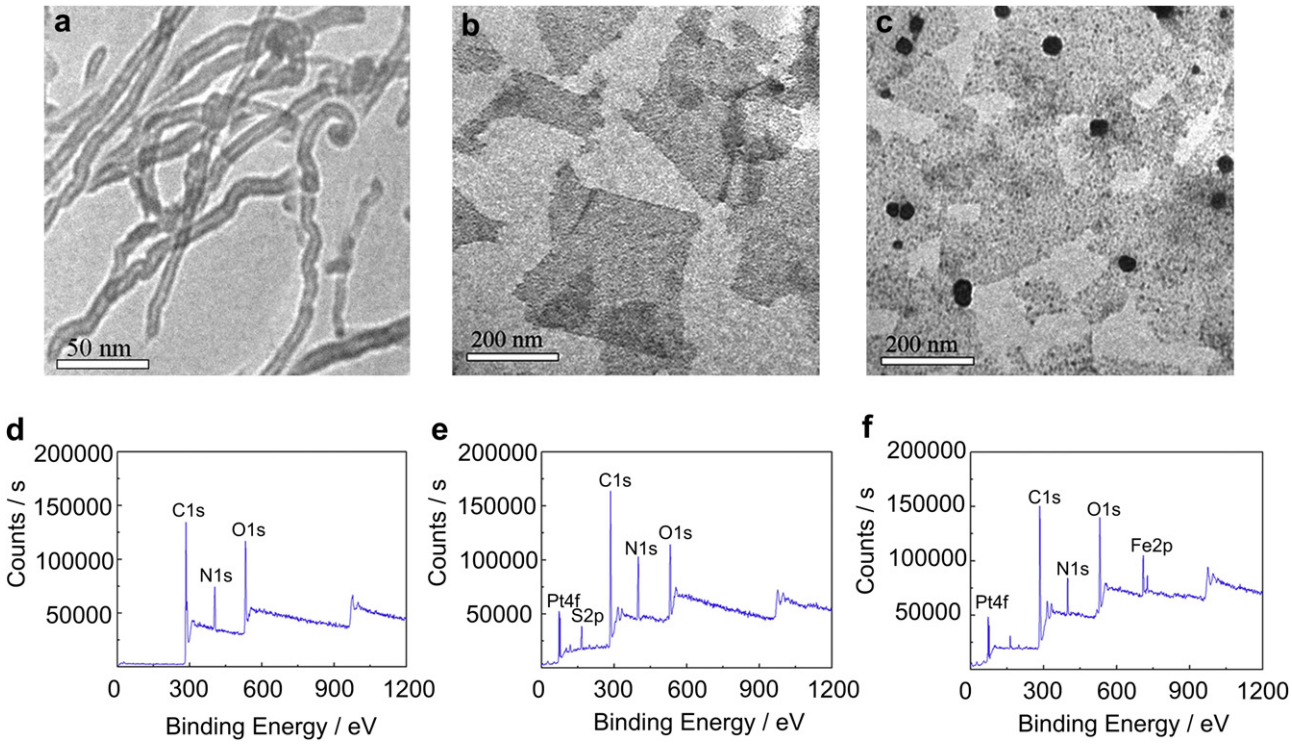

Fig. 2. TEM images of (a) SWCNTs, (b) rGS and (c) PtNPs-redox probes-rGS nanocomposites. XPS analysis of (d) rGS, (e) PtNPs-Tb-rGS nanocomposites and (f) PtNPs-Fc-rGS nanocomposites.

complementary pairing of aptamers and bulky analytes that retard the electron transfer tunnel.

3.3. Distribution effect of Apt I

To determine the suitable current response, distribution of Apt I (PBA and TBA) on the AuNPs@SWCNTs surface was studied. Fig. 4 showed the relationship between current response and the distribution of PBA and TBA. When proportion of one aptamer is larger, the corresponding current response is much higher than that of another aptamer. In order to make the current difference minor and keep the response signal relatively high, the same molar weight of PBA and TBA was adopted in this work.

3.4. Performance of the aptasensor

The amplification performance of the aptasensor was monitored by CV experiments. Fig. 5A showed the current response of the resulted aptasensor after the sandwich format reaction. Two pairs of stable and well-defined redox peaks (curve a) can be found, suggesting the efficient electroactivity of the redox probes-rGS bioconjugates labels. In order to evaluate whether or not the immobilized PtNPs and bienzyme have the catalysis ability, various concentrations of glucose were added into the solution. It can be readily seen that the reduction peaks enormously increased with the addition of glucose, indicating a typical electrocatalytic process of glucose and H_2O_2 (curve b).

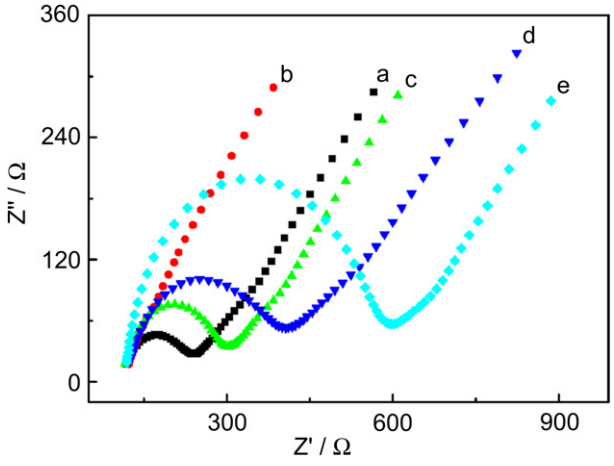

Fig. 3. EIS for each immobilized step in 5 mM $[Fe(CN)_6]^{4-/3-}$+0.1 M KCl solution: (a) bare GCE, (b) AuNPs@SWCNTs/GCE, (c) Apt I/AuNPs@SWCNTs/GCE, (d) HT/Apt I/AuNPs@SWCNTs/GCE, (e) analytes/HT/Apt I/AuNPs@SWCNTs/GCE.

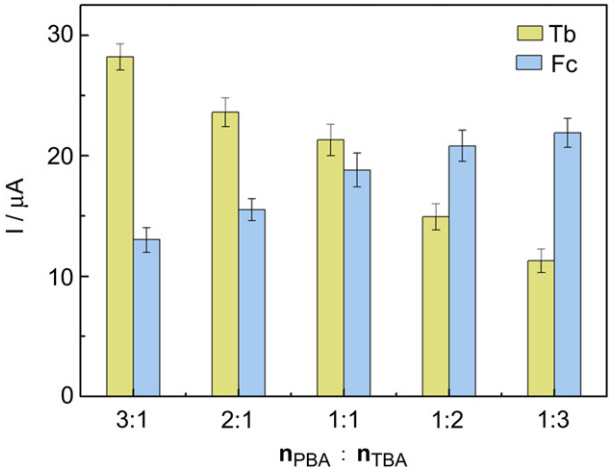

Fig. 4. Effect of molar ratio of the two Apt I (PBA to TBA) distribution on the AuNPs@SWCNTs surface.

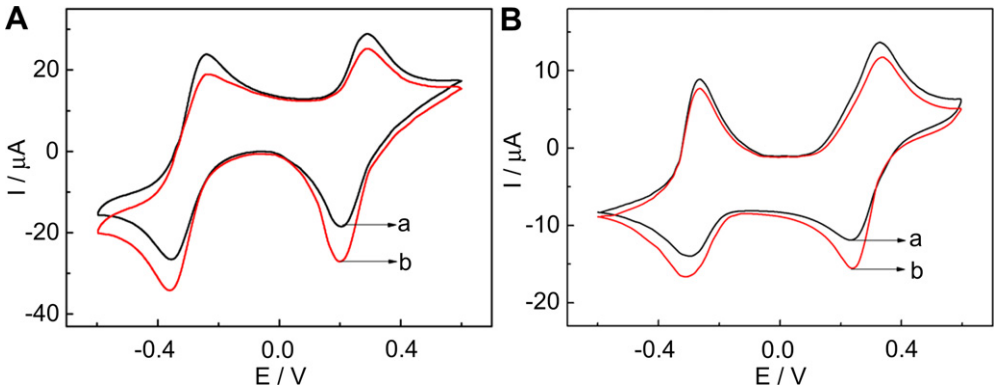

Fig. 5. CVs of the modified electrode using (A) multi-labeled PtNPs-redox probes-rGS nanocomposites and (B) multi-labeled rGS nanocomposites as tracers in the absence (a) and in the presence (b) of 3.6 mM glucose in PBS at a scan rate of 100 mV/s.

To further demonstrate the catalytic efficiency of PtNPs, electrochemical response of the modified electrode using multi-labeled rGS nanocomposites (redox probes, bienzyme and Apt II were all directly immobilized on rGS without PtNPs) as tracers was recorded (Fig. 5B). The peak current of redox probes (curve a) and the current increment with the addition of glucose (curve b) were both lower than that of the proposed aptasensor. It should be ascribed to the employment of PtNPs, which not only increased the immobilization of redox probes on rGS but also absorbed abundant enzyme onto their active surfaces, accordingly enhanced the electrochemical signals.

The signal amplification was also confirmed by DPV measurement. As shown in Fig. 6, a 2.5-fold increase in the catalytic current was observed at multi-labeled PtNPs-redox probes-rGS/analytes/Apt I/AuNPs@SWCNTs modified electrode (curve d) compared with redox probes labeled Apt II/analytes/Apt I/AuNPs@SWCNTs modified electrode (curve b), indicating rGS as a matrix could introduce masses of redox probes, PtNPs and bienzyme on the electrode surface. Similarly, the catalytic current obtained from multi-labeled PtNPs-redox probes-rGS/analytes/Apt I/AuNPs modified electrode (curve c) was 3-fold higher than that from redox probes labeled Apt II/analytes/Apt I/AuNPs modified electrode (curve a). The achieved amplification was mainly ascribed to the abundant PtNPs, GOD and HRP on rGS extremely amplified the electrochemical signals of redox probes through electrocatalytic reduction. In addition, compared analytes/Apt I/AuNPs modified electrode (curve c) with analytes/Apt I/AuNPs@SWCNTs modified electrode (curve d), the catalytic current increased about 6 μA when multi-labeled PtNPs-redox probes-rGS nanocomposites were used as the detection aptamers. Also, the responses increased approximate 4 μA when traditional redox probes labeled Apt II was used (curve a and b). These data illustrated that the presence of SWCNTs not only obviously increased the surface area to capture more aptamers on the electrode surface but also accelerated electron transfer. Based on the dual amplification of SWCNTs and multi-labeled PtNPs-redox probes-rGS nanocomposites, the catalytic current of the proposed aptasensor (curve d) enhance about 4-fold in comparison with that of redox probes labeled Apt II/analytes/Apt I/AuNPs modified electrode (curve a) without SWCNTs modification and rGS labeling.

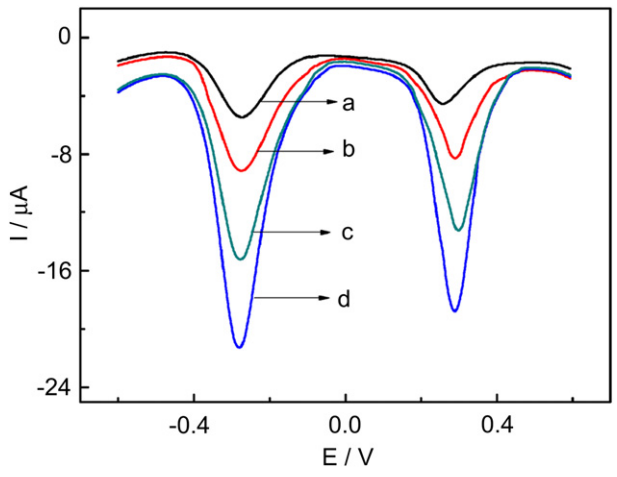

Fig. 6. DPV responses of the resulted aptasensors after the sandwich format reaction in 0.1 M PBS (pH 7.4) containing 3.6 mM glucose by using various sensor platforms and labels: (a) redox probes labeled Apt II and Apt I/AuNPs as sensor platform, (b) redox probes labeled Apt II and Apt I/AuNPs@SWCNTs as the sensor platform, (c) multi-labeled PtNPs-redox probes-rGS nanocomposites and Apt I/AuNPs as the sensor platform and (d) multi-labeled PtNPs-redox probes-rGS nanocomposites and Apt I/AuNPs@SWCNTs as the sensor platform.

To assess the performance of the proposed aptasensor, we measured routine samples of PDGF and thrombin with different concentrations using the developed sandwich-type with multi-labeled PtNPs-redox probes-rGS nanocomposites as tracers and glucose as substrate. The amperometric responses for simultaneous detection of PDGF and thrombin increased with the increment of PDGF and thrombin concentrations in the sample solution after the complementary pairing interaction (Fig. 7a). The calibration plots showed a good linear relationship between the reduction peak currents and the analytes concentrations in the ranges from 0.01 to 35 nM with a detection limit (defined as $DL = 3S_B/m$, where m is the slope of the corresponding calibration curve and S_B is the standard deviation of the blank) [31] of 8 pM for PDGF and 0.02 to 45 nM with a detection limit of 11 pM for thrombin, respectively (Fig. 7b and c). The detectable concentrations of PDGF and thrombin in the present work were comparable to the detection limits reported by the use of other methods, including 63 pM of PDGF based on specific target binding-induced rolling circle amplification [32] and 20 pM of thrombin taking AuNPs based sandwich sensing platform as a model [33]. The reason for the relatively low detection limits was that quite a number of redox probes, PtNPs and bienzyme conjugated onto rGS significantly enhanced the amperometric responses.

To evaluate the cross-reactivity of the multiplexed electrochemical assay, two control tests were carried out as follows (analytes concentrations of 0.1 nM and 15 nM were used as examples): (i) single analyte, PDGF or thrombin, was assayed using multi-labeled PtNPs-redox probes-rGS nanocomposites as signal tags; (ii) PDGF and thrombin were simultaneously monitored using

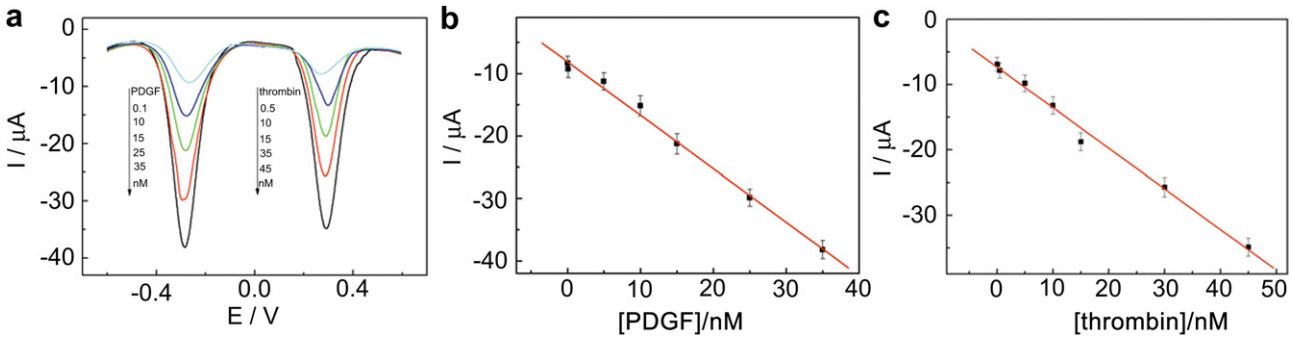

Fig. 7. (a) DPV responses of the proposed aptasensor after incubation with different concentration of PDGF and thrombin. Calibration curves for the simultaneous determination of PDGF and thrombin using (b) multi-labeled PtNPs-Tb-rGS nanocomposites and (c) multi-labeled PtNPs-Fc-rGS nanocomposites as tracers.

Table 1
Cross-reactivity level of the aptasensor.

sample type	concentration (nM)	current shift at PDGF position (μA)[a,b]	current shift at thrombin position (μA)[a,c]
PDGF	0.1	−5.4	−0.1
	15	−18.4	−0.2
thrombin	0.1	−0.1	−4.1
	15	−0.3	−15.6
PDGF + thrombin	0.1 + 0.1	−5.6	−3.9
	15 + 15	−18.1	−15.8

[a] The average value of three measurements.
[b] The background current was −3.8 μA at PDGF position.
[c] The background current was −3.2 μA at thrombin position.

multi-labeled PtNPs-redox probes-rGS nanocomposites as signal tags. The electrochemical responses were measured and the current shifts were displayed in Table 1. Significantly higher current shift was observed with the corresponding target analyte and extremely low current shift was observed with another one. The results indicated that the multiplexed detection exhibited low interference with each other and the cross-reactivity between the two analytes was negligible.

In order to illustrate the reproducibility of the aptasensor, five freshly prepared modified electrodes were incubated with 15 nM PDGF and 15 nM thrombin mixture. All five electrodes exhibited similar amperometric response behavior, and the relative standard deviation is 6.8%. This demonstrated that the reproducibility of the proposed aptasensor for PDGF and thrombin was acceptable.

4. Conclusions

In summary, we have successfully developed a novel electrochemical aptasensor for simultaneous detection of PDGF and thrombin using different redox probes as tracers. The higher sensitivity and wider linear range of the proposed aptasensor should be taken into account as the exhibition of AuNPs@SWCNTs and excellent electrocatalysis activities of PtNPs and bienzyme on rGS, which performed effective amplification properties as expected. Firstly, AuNPs@SWCNTs on electrode not only facilitated electrons transfer but also provided large accessible surface area for the immobilization of abundant Apt I. Secondly, rGS with high aspect ratio could increase the amount of redox probes, thus enhanced the response signals. Moreover, the synergistic reaction of PtNPs and bienzyme on rGS toward electrocatalyses could amplify the response signals of redox probes and improve the sensitivity. Besides, although the proposed technique was focused on the determination of PDGF and thrombin, it possessed the potential of wider application for other targets.

Acknowledgements

This work is supported by National Natural Science Foundation of China (21075100), Ministry of Education of China (708073), Specialized Research Fund for the Doctoral Program of Higher Education (20100182110015), State Key Laboratory of Electroanalytical Chemistry (SKLEAC 2010009) and Natural Science Foundation Project of Chongqing City (CSTC-2011BA7003,CSTC-2009BA1003).

References

[1] Huang CC, Huang YF, Cao ZH, Tan WH, Chang HT. Aptamer-modified gold nanoparticles for colorimetric determination of platelet-derived growth factors and their receptors. Anal Chem 2005;77:5735–41.
[2] Wang Y, Luo W, Reiser G. Trypsin and trypsin-like proteases in the brain: proteolysis and cellular functions. Cell Mol Life Sci 2008;65:237–52.
[3] Yang H, Ji J, Liu Y, Kong JL, Liu BH. An aptamer-based biosensor for sensitive thrombin detection. Electrochem Commun 2009;11:38–40.
[4] Zhu CL, Lu CH, Song XY, Yang HH, Wang XR. Bioresponsive controlled release using mesoporous silica nanoparticles capped with aptamer-based molecular gate. J Am Chem Soc 2011;133:1278–81.
[5] Bi S, Zhang JL, Zhang SS. Ultrasensitive and selective DNA detection based on nicking endonuclease assisted signal amplification and its application in cancer cell detection. Chem Commun 2010;46:5509–11.
[6] Xu W, Xue XJ, Li TH, Zeng HQ, Liu XG. Ultrasensitive and selective colorimetric DNA detection by nicking endonuclease assisted nanoparticle amplification. Angew Chem Int Ed 2009;48:6849–52.
[7] Feng LY, Chen Y, Ren JS, Qu XG. A grapheme functionalized electrochemical aptasensor for selective label-free detection of cancer cells. Biomaterials 2011; 32:2930–7.
[8] Du Y, Chen CG, Li BL, Zhou M, Wang EK, Dong SJ. Layer-by-layer electrochemical biosensor with aptamer-appended active polyelectrolyte multilayer for sensitive protein determination. Biosens Bioelectron 2010;25: 1902–7.
[9] Xiao Y, Piorek BD, Plaxco KW, Heeger AJ. A reagentless signal-on architecture for electronic, aptamr-based sensors via target-induced strand displacement. J Am Chem Soc 2005;127:17990–1.
[10] Deng CY, Chen JH, Nie Z, Wang MD, Chu XC, Chen XL, et al. Impedimetric aptasensor with femtomolar sensitivity based on the enlargement of surface-charged gold nanoparticles. Anal Chem 2009;81:739–45.
[11] Wang J, Meng WY, Zheng XF, Liu SL, Li GX. Combination of aptamer with gold nanoparticles for electrochemical signal amplification: application to sensitive detection of platelet-derived growth factor. Biosens Bioelectron 2009;24: 1598–602.
[12] Du Y, Li BL, Wei H, Wang YL, Wang EK. Multifunctional label-free electrochemical biosensor based on an integrated aptamer. Anal Chem 2008;80: 5110–7.
[13] Li XM, Liu JM, Zhang SS. Electrochemical analysis of two analytes based on a dual-functional aptamer DNA sequence. Chem Commun 2010;46:595–7.
[14] Song ZJ, Yuan R, Chai YQ, Zhuo Y, Jiang W, Su HL, et al. Horseradish peroxidase-functionalized Pt hollow nanospheres and multiple redox probes as trace labels for a sensitive simultaneous multianalyte electrochemical immunoassay. Chem Commun 2010;46:6750–2.
[15] Chang HX, Tang LH, Wang Y, Jiang JH, Li JH. Graphene fluorescence resonance energy transfer aptasensor for the thrombin detection. Anal Chem 2010;82: 2341–6.
[16] He SJ, Song B, Li D, Zhu CF, Qi WP, Wen YQ, et al. A graphene nanoprobe for rapid, sensitive, and multicolor fluorescent DNA analysis. Adv Funct Mater 2010;20:453–9.

[17] Shan CS, Yang HF, Han DX, Zhang QX, Ivaska A, Niu L. Water-soluble grapheme covalently functionalized by biocompatible poly-L-lysine. Langmuir 2009;25:12030–3.
[18] Kong BS, Geng JX, Jung HT. Layer-by-layer assembly of grapheme and gold nanoparticles by vacuum filtration and spontaneous reduction of gold ions. Chem Commun; 2009:2174–6.
[19] Guo SJ, Dong SJ, Wang EK. Three-dimensional Pt-on-Pd bimetallic nanodendrites supported on grapheme nanosheet: facile synthesis and used as an advanced nanoelectrocatalyst for methanol oxidation. ACS Nano 2010;4:547–55.
[20] Dreyer DR, Jia HP, Bielawski CW. Graphene oxide: a convenient carbocatalyst for facilitating oxidation and hydration reactions. Angew Chem Int Ed 2010;49:6813–6.
[21] Lu CH, Li J, Lin MH, Wang YW, Yang HH, Chen X, et al. Amplified aptamer-based assay through catalytic recycling of the analyte. Angew Chem Int Ed 2010;49:8454–7.
[22] Zhu CZ, Guo SJ, Fang YX, Dong SJ. Reducing sugar: new functional molecules for the green synthesis of grapheme nanosheets. ACS Nano 2010;4:2429–37.
[23] Zhong ZY, Wu W, Wang D, Wang D, Shan JL, Qing Y, et al. Nanogold-enwrapped grapheme nanocomposites as trace labels for sensitivity enhancement of electrochemical immunosensors in clinical immunoassays: carcinoembryonic antigen as a model. Biosens Bioelectron 2010;25:2379–83.
[24] Cao LY, Liu YL, Zhang BH, Lu LH. In situ controllable growth of prussian blue nanocubes on reduced graphene oxide: facile synthesis and their application as enhanced nanoelectrocatalyst for H_2O_2 reduction. ACS Appl Mater Interfaces 2010;2:2339–46.
[25] Yang MH, Javadi A, Li H, Gong SQ. Ultrasensitive immunosensor for the detection of cancer biomarker based on graphene sheet. Biosens Bioelectron 2010;26:560–5.
[26] You TY, Niwa O, Tomita M, Hirono S. Characterization of platinum nanoparticle- embedded carbon film electrode and its detection of hydrogen peroxide. Anal Chem 2003;75:2080–5.
[27] Polsky R, Gill R, Kaganovsky L, Willner I. Nucleic acid-functionalized Pt nanoparticles: catalytic labels for the amplified electrochemical detection of biomolecules. Anal Chem 2006;78:2268–71.
[28] Ipe B, Yoosaf K, Thomas KG. Functionalized gold nanoparticles as phosphorescent nanomaterials and sensors. J Am Chem Soc 2006;128:1907–13.
[29] Jana NR, Ying JY. Synthesis of functionalized Au nanoparticles for protein detection. Adv Mater 2008;20:430–4.
[30] Iijima S, Ichihashi T. Single-shell carbon nanotubes of 1-nm diameter. Nature 1993;363:603–5.
[31] Radi AE, Sánchez JL, Baldrich E, O'Sullivan CK. Reagentless, reusable, ultrasensitive electrochemical molecular beacon aptasensor. J Am Chem Soc 2006;128:117–24.
[32] Wu ZS, Zhou H, Zhang SB, Shen GL, Yu RQ. Electrochemical aptameric recognition system for a sensitive protein assay based on specific target binding-induced rolling circle amplification. Anal Chem 2010;82:2282–9.
[33] Li BL, Wang YL, Wei H, Dong SJ. Amplified electrochemical aptasensor taking AuNPs based sandwich sensing platform as a model. Biosens Bioelectron 2008;23:965–70.